

AperTO - Archivio Istituzionale Open Access dell'Università di Torino

**Multicolor immunochromatographic strip test based on gold nanoparticles for the determination of aflatoxin B1 and fumonisins**

**This is a pre print version of the following article:**

*Original Citation:*

*Availability:*

This version is available <http://hdl.handle.net/2318/1632654> since 2020-03-16T18:26:39Z

*Published version:*

DOI:10.1007/s00604-017-2121-7

*Terms of use:*

Open Access

Anyone can freely access the full text of works made available as "Open Access". Works made available under a Creative Commons license can be used according to the terms and conditions of said license. Use of all other works requires consent of the right holder (author or publisher) if not exempted from copyright protection by the applicable law.

(Article begins on next page)



# UNIVERSITÀ DEGLI STUDI DI TORINO

***This is an author version of the contribution published on:***

*Questa è la versione dell'autore dell'opera:*

*F.Di Nardo, C.Baggiani, C.Giovannoli, G.Spano, L.Anfossi: "Multicolor immunochromatographic strip test based on gold nanoparticles for the determination of aflatoxin*

*B1 and fumonisins" Microchim.Acta, 2017, 184, 1295-304 (DOI 10.1007/s00604-017-2121-7)*

***The definitive version is available at:***

*La versione definitiva è disponibile alla URL:*

*<http://www.springer.com/chemistry/analytical+chemistry/journal/216>*

## **Multicolor immunochromatographic strip test based on gold nanoparticles for the determination of aflatoxin B1 and fumonisins**

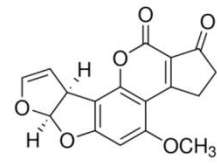
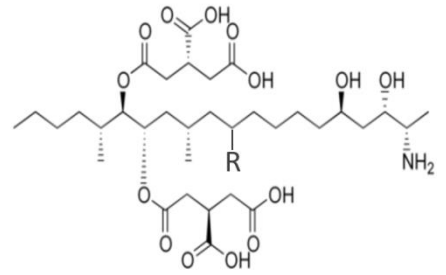
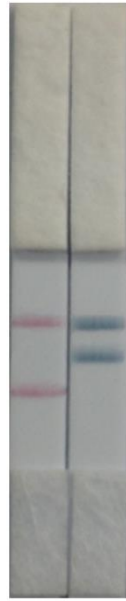
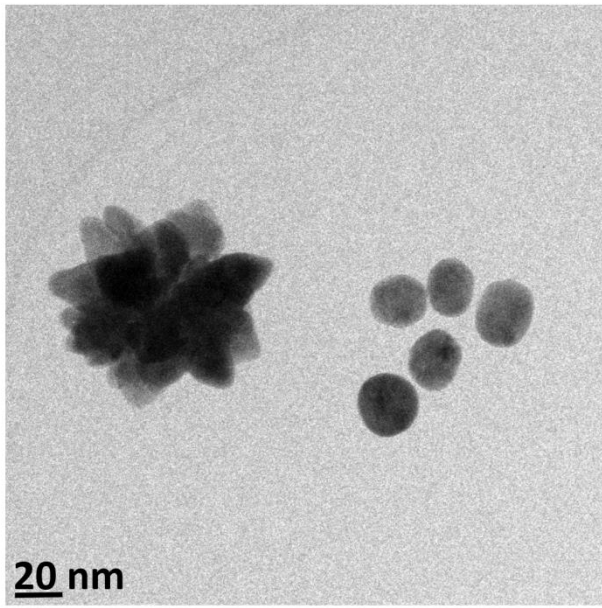
Fabio Di Nardo, Claudio Baggiani, Cristina Giovannoli, Giulia Spano, Laura Anfossi\*

Department of Chemistry, University of Turin. Via Giuria, 5, I-10125 Turin, Italy

\*to whom correspondence should be addressed. Tel: +390116705219, fax: +390116705242. E-mail: [laura.anfossi@unito.it](mailto:laura.anfossi@unito.it)

### **Graphical abstract**

Blue desert rose-like gold nanoparticles (DR-GNPs) were synthesized, characterized and applied as label for the ImmunoChromatographic Strip Test (ICST) technique, in which red spherical GNPs (s-GNPs) are usually employed. The combined use of the blue DR-GNP and red s-GNPs allowed developing of an intuitive multicolor ICST for the simultaneous detection of Aflatoxin B1 and Fumonisins in maize flour.



## Abstract

Desert rose-like gold nanoparticles (DR-GNPs) that exhibited a blue color due to the plasmon resonance band at 620 nm were prepared. The blue DR-GNPs were obtained through a seeding growth approach and characterized by UV-vis spectroscopy, transmission electron microscopy and dynamic light scattering. The DR-GNPs had a hydrodynamic diameter of ~72 nm and were used as labels for the antibody in an immunochromatographic strip test (ICST). Although the particular shape of DR-GNPs and their higher surface area with respect to spherical GNPs, they demonstrated to be effective as antibody labels. A multicolor ICST for aflatoxin B1 and fumonisins was developed that employs both blue DR- and red spherical GNPs. The multicolor ICST allows for simultaneous rapid determination of the two mycotoxins in maize flour, with visual cut-off levels at  $2 \mu\text{g kg}^{-1}$  for aflatoxin B1 and  $1000 \mu\text{g kg}^{-1}$  for fumonisins.

**Keywords:** Non-spherical gold nanoparticles, Labels for Immunoassay, Lateral flow Assay, Aflatoxin B1, Fumonisins, Maize

## Introduction

During the last decades, noble metal nanoparticles (NPs) have increased the breadth of their impact and are now becoming a backbone of modern technology. Their applications range from biomedical, electronics, catalysis, sensing of organic and inorganic molecules, to optical devices and many others [1].

Gold nanoparticles (GNPs) are one of the most popular [2] and widely used NPs as sensitive probes for colorimetric sensors thanks to the strong surface plasmon resonance (SPR) in the visible spectroscopy region, and to their high extinction coefficients. Moreover, since the SPR band is very sensitive to changes in refractive index and dispersion state of GNPs, most of GNPs-based colorimetric assays rely on the color change from red to purple-blue when GNPs aggregate [3-5].

The immunochromatographic strip test (ICST), also known as Lateral Flow Immunoassay, is one of the most successful colorimetric assay because of the advantages of simplicity, rapidity, cost-effectiveness and no requirement of equipment or technical expertise for operation. The ICST is based on immunoassays in which the sample and a suitable labeled probe flow by capillary forces along an analytical porous membrane that contains immobilized reagents with molecular recognition properties. These are placed in specific areas of the membrane, that are usually defines as Test and Control lines, where the former gives information about the target analyte, while the latter ensures the correct functioning of the test. The occurring of immunoreactions leads to the

development of detectable bands in correspondence of the Test and Control lines, due to the accumulation of the label in such zones.

Typically, colorimetric ICSTs employ spherical GNPs (s-GNPs), with diameter comprises between 20 and 40 nm, as labels. These nanoparticles exhibit a deep-red color, which reflects their SPR band around 525 nm [6-9] and allow for the naked-eye detection of ICST result when accumulated on the lines. Usually, the visual inspection of the color of the lines provides a qualitative result (“yes/no” response, fig. 1); even if semi-quantitative tests can be designed, as well [8-9].

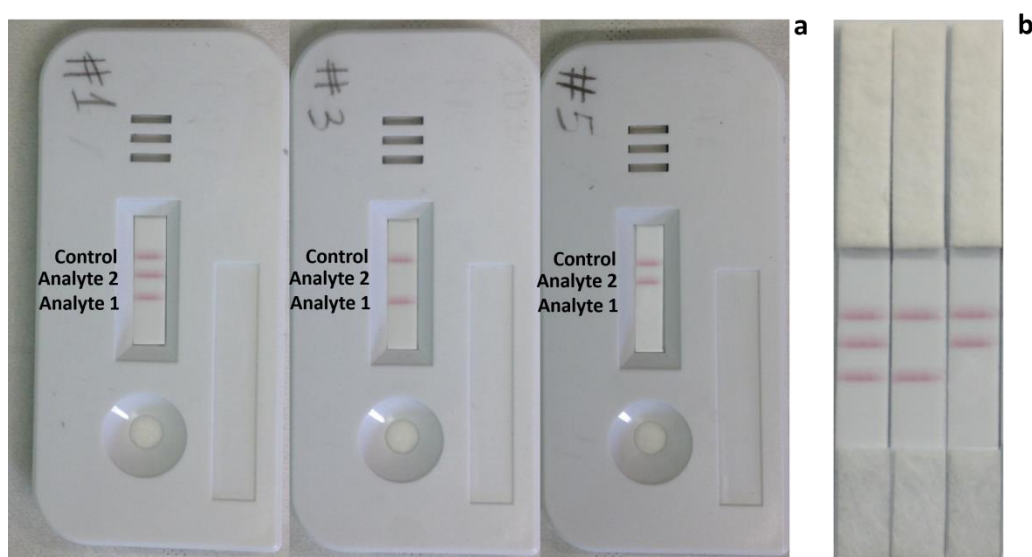


**Fig. 1.** Exemplification of a multiplex ICST employing s-GNP (a) in cassette format. (b) in dipstick format

Besides common spherical GNPs, some authors reported the use of non-spherical [10-11] and multilayer GNPs [12-13] as labels for ICSTs with the aim of improving the assay sensitivity. More specifically, Ji *et al.* used multi-branched GNPs as labels for developing an ICST for the detection of Aflatoxin B1, and reported higher optical brightness, better colloidal stability and better sensitivity than using s-GNPs [11]. These multi-branched GNPs exhibited a blue color instead of the red color of s-GNPs, because the size and shape of GNPs have significant influences on the SPR band.

In order to exploit the blue color of the multi-branched GNPs for the development of an intuitive ICST designed for multianalyte analysis (fig. 2), the present study reports the synthesis of desert rose-like GNPs (DR-GNPs), their characterization by means of UV-vis absorption spectroscopy, transmission electron microscopy (TEM) and dynamic light scattering (DLS) and their use as labels for ICST. Although other ligands have been reported, such as for example aptamers [14-15], the large majority of GNP-based ICSTs reported in the literature and commercially available use antibodies as recognition elements [16-17] and most frequently the labeling of antibodies with

GNPs is achieved through passive adsorption of proteins on their surfaces. Therefore, a preliminary study on the passive adsorption of antibodies on DR-GNPs as a function of the pH and the amount of antibody (Ab) used for conjugation with DR-GNP was conducted. Both the stability of the sol and the performance of the labeled antibodies in a model ICST, in terms of signal intensities and analytical sensitivity, were considered.

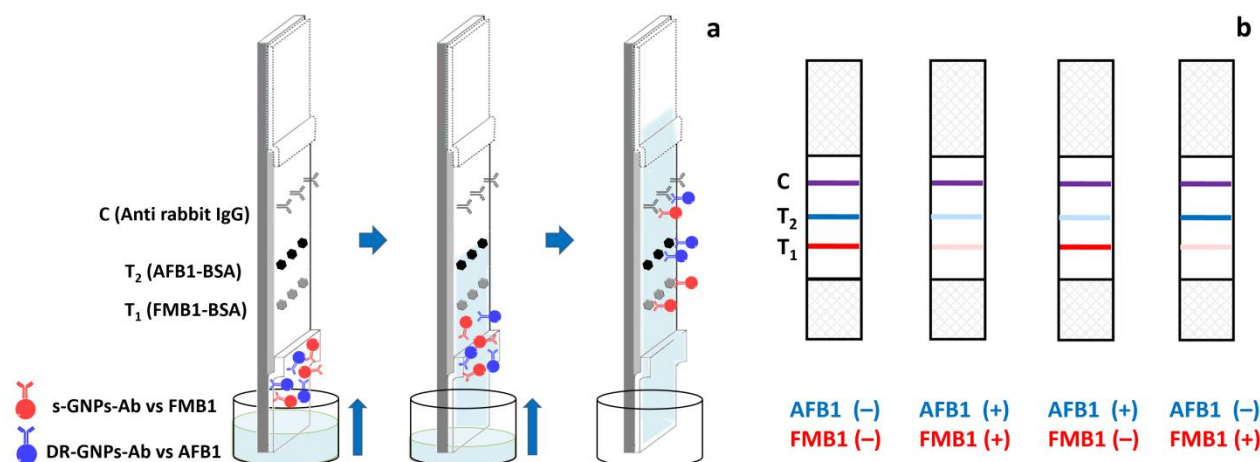


**Fig. 2.** (a) Scheme of the multicolor-ICST in dipstick format, based on the simultaneous use of s- and DR-GNPs. (b) Scheme of the naked-eye interpretation of the results: when the red (blue) intensity of the Test line is significantly weaker than that of the negative reference, the sample is assigned as positive for FMB1 (AFB1) contamination

Furthermore, the peculiar spectral properties of the DR nanoparticles allowed for designing a multiplexed ICST for the simultaneous detection of two food contaminants. The multiplex analysis is highly desirable in screening system for food safety assessment since it allows the on-site detection of several targets within a single analysis, providing significant savings in terms of time and operating costs [18]. The ICST technique offers easy implementation of multiplex analysis, thus allowing producing very attractive cost-effective screening tools. In multiplex ICST two or more Test lines are dispensed on the membrane, allowing the simultaneous detection of respective targets in a single test. Usually, multiplex ICST are enclosed in a plastic cassette on which reference to the targets is provided in correspondence to the position of each Test line (fig. 1a). Otherwise, multiplex ICSTs in dipstick format cannot provide any indication about lines positioning (fig. 1b) that makes their interpretation confusing, and strongly limits their applicability.

However, ICSTs in dipstick format are largely preferred with respect to the cassette format, because their production is more simple and cheaper. In this context, assigning different colors to different analytes would make easier and more intuitive the visual interpretation of the results provided by a multiplex dipstick ICST. Color-encoded ICSTs in the multiplex format have been described, which

exploit the unique spectral characteristics of quantum dots (QDs) [19-20]. These inorganic nanocrystals are capable of emitting fluorescent light at different wavelengths depending on their size and composition, when excited by the same source. Therefore, Taranova et al. used QDs emitting at different wavelengths for labeling three antibodies and simultaneously determining three classes of antibiotics by a multiplex ICST [19]. Similarly, Foubert et al. used three differently emitting QDs for labeling as many antibodies and to set an ICST for the multiple determinations of four mycotoxins [20]. Although QDs are particularly suited for multiplexing because of the tunable color of the emitted fluorescence, still they require a light source for excitation, thus limiting the portability and cost-effectiveness of QD-based ICSTs. Metal nanoparticles also offer the opportunity of tailoring the SPR band (and thus the color) by varying NP dimension and shape [21-22]. In fact, the advantage of using differently shaped and therefore differently colored silver nanoparticles as labels for multiplex ICST has been demonstrated by Yen et al. [23]. The authors reported an ICST for the simultaneous detection of three viruses, which was easily interpreted by the naked-eye through color-encoding and without needing any supplementary equipment.

Here the first multicolor ICST based on the use of gold nanoparticles with different colors and, namely blue DR-GNP and red s-GNPs, is described and typified by the simultaneous detection of aflatoxin B1 (AFB1) and Fumonisin (FMs) as a model system. AFB1 is a mycotoxin mainly produced by *Aspergillus* species, toxigenic fungi growing on several agricultural products, including maize; it has been classified as human carcinogens (Group 1) by the International Agency for Research on Cancer (IARC) [24]. Due to adverse effects of AFB1 and to its incidence in food, the European Union has set a  $2 \mu\text{g Kg}^{-1}$  maximum allowed level for AFB1 for all cereals and all products derived from cereals, including processed cereals products [25]. FMs are mycotoxins mainly produced by *Fusarium* fungi, which also grow on agricultural commodities in the field, at the harvest or during the storage [26]. FMs contamination is endemic in the central Europe and has been assessed mainly in maize [27]. These mycotoxins have been classified as possible human carcinogens (Group 2B) by the IARC [28] and, as for the AFB1, principal FMs (namely, fumonisin B1, FMB1, and fumonisin B2, FMB2) are regulated by European Union [29] and their monitoring is mandatory for food safety assessment. AFB1 and FMs are found in several commodities, including cereals, and their co-occurrence has already been demonstrated [30-31]. Furthermore, the possible synergistic effect of different mycotoxins on human and animal health has been underlined [30-31]. Therefore, the availability of analytical devices aimed at detecting co-occurring mycotoxins are strongly demanded for monitoring the entire production chain, according to the Hazard Analysis and Critical Control Points (HACCP) procedures.



## Experimental

### *Preparation of DR-GNPs*

Non-spherical GNPs were synthesized through a seeding growth approach, as described by Li *et al.* [21] and Ji *et al.* [11] with slight modification. Small s-GNPs (SPR band at 518 nm corresponding to a mean diameter of approximately 11 nm) were used as the seeds and a mixture of HAuCl<sub>4</sub>, sodium citrate and hydroquinone as the growth solution. It is somewhat unclear if the growth of the branch is dominated by the epitaxial mechanism or by the random attachment of the small GNPs on the seeds surface [22], however, the hypothesis is the occurring stepwise reduction of Au<sup>III</sup> to Au<sup>I</sup> by citrate and Au<sup>I</sup> to Au<sup>0</sup> by hydroquinone [21].

DR-GNPs with a SPR band at 620 nm and a hydrodynamic diameter of about 72 nm were prepared as follow: in ultrapure water,  $1.9 \times 10^{-8}$  mol of tetrachloroauric acid was mixed with  $9.3 \times 10^{-13}$  mol of s-GNP seeds (mean diameter of 11 nm) at room temperature. Then,  $7.5 \times 10^{-9}$  mol of sodium citrate was added to the mixture, which was stirred for 2 min for homogenization. Finally,  $3.0 \times 10^{-5}$  mol of hydroquinone was rapidly added to the solution under vigorous stirring. The solution was kept under stirring at room temperature for further 20 min and the sol exhibits a blue color, which is consistent with the SPR band observed. The sol was adjusted to the desired pH with carbonate buffer (sodium carbonate-sodium bicarbonate 50 mM, pH 9.6).

### *Preparation of s-GNP-labeled antibodies*

The antibodies were labeled with s-GNPs as previously described [32] through the adsorption of proteins onto GNPs surface. The s-GNPs were adjusted to the desired pH with carbonate buffer and the amount of Ab defined from the titration was added to 1 mL of s-GNPs. After 30 min at 37°C, 100  $\mu$ L of borate buffer (20 mM pH 8.0) supplemented with 1% w/v BSA was added and the solution kept at 37°C for further 10 min. The mixture was centrifuged for 10 min at 25°C (18400 x g) and the pellet was washed twice by re-suspension in borate buffer with 0.1% BSA added and borate buffer with 1% w/v BSA, 2% w/v sucrose, 0.25% v/v Tween 20, and 0.02 % sodium azide. Finally, the pellets were pooled and stored at 4°C until use.

### *Preparation of DR-GNP-labeled polyclonal antibodies*

Also the DR-GNP-labeled antibodies were prepared through adsorption by adding the amount of Ab defined from the titration to 1 mL of pH-adjusted DR-GNPs. However, the conjugation protocol was modified as follows: borate buffer supplemented with 10% BSA was used, the centrifugation

was conducted for 15 min at 4°C and 6800 x g and the pellet was directly re-suspended in borate buffer with 1% BSA added without washings.

#### *Assay procedure*

The s-GNPs-, DR-GNPs- and multicolor-ICST in dipstick format were carried out at room temperature. 60 µL of sample extracts (or AFB1 and FMB1 standards) were transferred into wells of a 96-well microtiter plate (VWR International, Milan, Italy, <https://it.vwr.com/store/>). The strip was dipped in the well to start the capillary migration process (fig. 2a). Strips were composed of - from bottom to top - a glass fiber pad, which acted as the reservoir for GNPs conjugated to antibodies and also as the sample pad; the nitrocellulose membrane, which comprised two Test lines (T1 responsive to FMs and T2 to AFB1, respectively) and a Control line; and a cellulose fiber pad as the adsorbent pad. After 10 min, test results were qualitatively estimated by the naked-eye and, if necessary, quantitatively evaluated by acquiring strip images in order to obtain the optical intensities of the lines. In this case, images were processed with QuantiScan 3.0 software (Biosoft, Cambridge, UK, [www.biosoft.com/](http://www.biosoft.com/)).

Result evaluation was based on the comparison of the color intensities of Test lines with those furnished by a negative sample (fig. 2b), while the Control line ensured the validity of the test.

#### *Analytical performances of the multicolor-ICST*

The multicolor ICST was designed as an intuitive visual ICST for multianalyte detection; therefore its analytical performances as a qualitative test were calculated. The visual limit of detection (vLOD) of the test was determined by analyzing standard solutions of each target mycotoxin diluted in the running buffer (phosphate buffer containing 1% BSA and 0.1% Tween 20) or in blank maize extract. The vLOD was defined as the lowest AFB1 and FMB1 concentrations resulting in a Test line color significantly weaker than that of the respective line given by a negative sample. Each standard was measured at least in triplicate and the visual observation was conducted by three different subjects. The vLOD obtained in maize extract was also established as the cut-off level to distinguish positive samples from negative samples. The precision and the accuracy of the test were evaluated on fortified samples, verifying that the Test lines of eight replicates were similar to each other, but different from the Test line of the negative sample. The cut-off levels, defined as above described, were used as fortification levels. The accuracy of the multicolor ICST was also evaluated by analyzing real samples and verifying the capability of the test to distinguish between negative (< cut-off level) and positive samples ( $\geq$  cut-off level). Validity of the multicolor ICST was checked

on 18 naturally contaminated maize flour samples by calculating the diagnostic sensitivity, specificity, and efficiency, and the positive and negative predictive values.

#### *Analysis of maize flour samples*

Maize flour samples were obtained directly from producers or mills and were stored at -20°C. Their content in fumonisins (intended as the sum of fumonisins B1, FMB1 and fumonisins B2, FMB2) was determined by the LC-MS/MS, as previously described [32], while the AFB1 contamination was assessed by a commercial ELISA kit (EuroClone SpA, Milano, Italy, <http://www.euroclonegroup.it/>). A methanol-water solution (50:50, v/v) was used to extract mycotoxins from maize flour (5 mL of extracting solution per 1 g of sample). After a 2 min manual shaking, the suspension was allowed to settle for 5 min and the supernatant was analyzed or used to prepare FMB1 and AFB1 calibrators. Matrix interference and the high methanol content caused a significant decrease of lines intensities, affecting the visual interpretation of the result. In order to minimize this effect, we diluted the extracts 1+1 with the running buffer prior to analysis. Calibrators were prepared daily by diluting the reference AFB1 and FMB1 solutions with the extract of blank maize flour, i.e.: which FMs and AFB1 content resulted undetectable according with the reference measurements.

## **Results and discussion**

#### *GNPs characterization*

Spherical gold nanoparticle of putative diameter comprised between 20 and 40 nm (s-GNPs) were synthesized using the citrate reduction method [32], while multi-branched desert rose-like gold nanoparticles (DR-GNPs) were prepared using a seeding growth approach adapted from that previously reported by Ji et al. [11]. TEM analysis allowed to visualize GNP morphology: s-GNPs showed the expected spherical shape (Fig. 3 b), while DR-GNPs showed a central core decorated with several branches (fig. 3 d). The size of the s-GNPs was calculated from TEM micrographs resulting in a mean diameter of 25 nm (fig. S1).

Given the non-spherical shape of the DR-GNPs, their dimension was measured by DLS that showed a unimodal size distribution, with a mode hydrodynamic diameter of ~ 72 nm (60 nm corresponded to the 10<sup>th</sup> percentile and 87 nm to the 90<sup>th</sup> percentile, data not shown).

UV-vis spectra of s- and DR- GNPs showed strong SPR bands, with  $\lambda_{\text{max}}$  at 525 and 620 nm, respectively (fig. 3 a, c). According to Khlebstov [33], is also possible to estimate the diameter of

spherical GNP directly from their  $\lambda_{\max}$ . The model furnished a mean diameter of 30.5 nm for the s-GNP with  $\lambda_{\max}$  of 525 nm, which slightly differs from the value obtained from TEM micrographs.

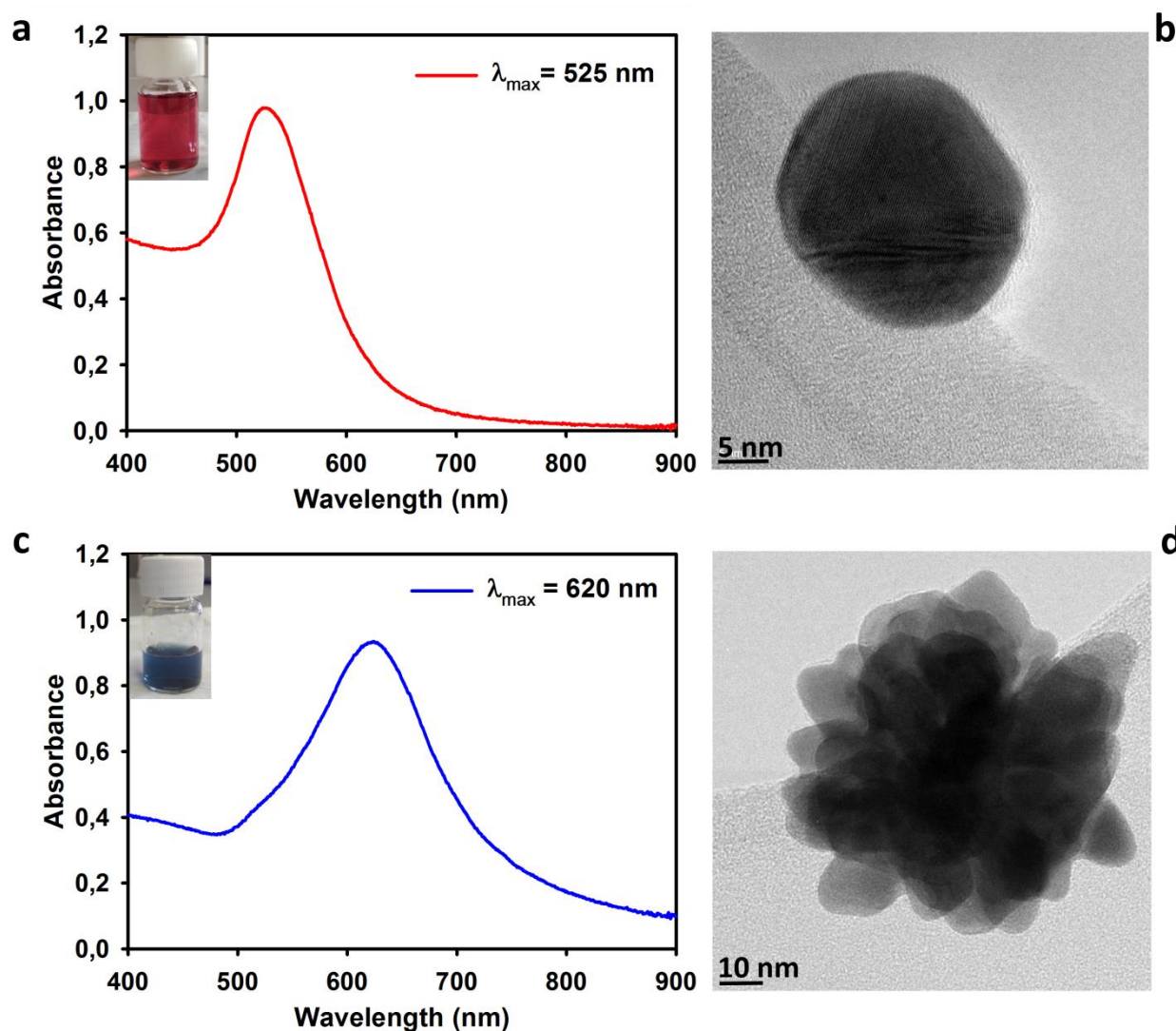


**Fig. 1.** (a) Visible spectrum of s-GNPs. Inset: picture of the s-GNP solution. (b) TEM micrograph of s-GNPs obtained at 500000 x magnification. (c) Visible spectrum of DR-GNPs. Inset: picture of the DR-GNP solution. (d) TEM micrograph of DR-GNPs obtained at 200000 x magnification

#### *S- and -DR-GNPs behavior during conjugation with antibodies*

Regardless of their dimension and shape, both s- and DR-GNPs were obtained from synthetic routes that produced metal NPs capped with citrate, so a similar interaction mechanism for the adsorption of antibodies on their surfaces was supposed. Proteins (and particularly, immunoglobulins) spontaneously adhere to the surface of colloidal gold nanoparticles capped with citrate through several types of non-covalent interactions such as the attraction between hydrophobic parts of the protein and the metal surface and the electrostatic interactions between positively charged amino

acids and N-terminus of the protein and the negatively charged surface of the citrate-capped particles [34].

The labeling of antibodies with GNPs for developing GNP-based ICST requires to define the minimum amount of the antibody to be adsorbed by nanoparticles in order to stabilize the nanoparticles themselves, which depends on the specific antibody used [7, 34-35].

Usually, the optimum amount of antibody (Ab) for labeling with GNPs is defined as the minimum amount preventing GNP aggregation upon addition of a concentrated salt (e.g. 10% sodium chloride) and is established by visually inspecting the color of GNP-Ab solutions after salt addition. In fact, GNPs aggregation determines a shift of the SPR band from red towards purple or even blue-grey for highly aggregated GNPs.

To investigate the influence of the morphology of the DR-GNPs on its colloidal stability, also as compared to s-GNP, a polyclonal rabbit antibody directed towards aflatoxin B1 was used as a model system for being conjugated to both kinds of nanoparticles. As expected, a higher amount of Ab was needed to prevent GNP flocculation in the case of DR-GNPs because of their higher surface area: 2  $\mu\text{g}$  of antibodies was sufficient to stabilize 0.5 ml of s-GNPs while 8  $\mu\text{g}$  were needed for shielding the same amount of DR-GNPs. For DR-GNPs the flocculation induced by salt addition shifted the SPR band over the UV-vis range, causing the blue color of the sol turning to colorless with a gradual decrease of the OD (Fig. S2). TEM images confirmed that the colorless sol obtained for insufficient amount of antibodies adsorbed corresponded to aggregated DR-GNPs (inset figure S2 b).

Using the respective stabilizing amounts of the protein, two conjugates of the anti-AFB1 antibody were prepared with s-GNPs and DR-GNPs, respectively. UV-vis measurements were used to confirm the effective adsorption of antibodies onto s- and DR-GNPs, since the formation of a layer of protein on the GNP surface causes the modification of the refractive index and a shift of the SPR band. Accordingly, a  $\lambda_{\text{max}}$  shifts from 525 nm to 530 nm for s-GNPs and from 620 nm to 630 nm for DR-GNPs were recorded and were considered as indicating successful conjugation.

Conjugation of DR-GNPs with antibodies required some minor modifications of the usual protocol employed for s-GNPs-Ab conjugation. In details, a higher amount of BSA was requested to block any unreacted sites on the DR-GNPs after coating with the antibody due to the increased superficial area of the DR-GNP compared to s-GNP. Furthermore, lower temperature and lower centrifugal force should be employed in order to avoid aggregation phenomena. This finding apparently indicated that DR-GNPs were more prone to aggregation compared to s-GNPs. However, it should be noted that colloidal s-GNPs of diameter comparable to that of DR-GNP are decidedly less stable [11], so, conversely, the particular shape of the DR-GNPs contributes in stabilizing the colloid.

As a general rule, it is considered that for maximizing the interaction of a protein with GNPs, conjugation should be conducted adjusting the pH at approximately 0.5 pH unit above the isoelectric point of the protein to be conjugated [36]. However, a fine-tuning of the system is recommended by determining the optimal pH value for conjugation for each specific antibody to each GNP preparation in order to maximize the sensitivity of the resulting assay [35, 37]. Accordingly, GNPs were conjugated to the stabilizing amounts of antibody (as previously determined) while varying the pH of the sol from 5 to 8. The GNP-Ab conjugates were used to set a preliminary immunochromatographic test for measuring AFB1. ICSTs were carried out by quantitatively measuring the color intensity of the Test and Control lines for three levels of AFB1 (0-1-10 ng ml<sup>-1</sup>); furthermore, for each pH value, three different concentrations of the GNP-Ab conjugate were employed, reported as OD values (0.5-1-2).

Because AFB1 is a small molecule characterized only by one epitope, the competitive format was applied for its detection. In the competitive assay, the free antigen in solution and the antigen immobilized on the Test line compete for binding to the GNP-labeled antibody. In the presence of the target AFB1 in the sample, GNP-labeled antibodies bind to it while the binding to the reagent on the Test line is inhibited proportionally. Thus, the color intensity due to GNP accumulation on the Test line is lower compared to that observed for a blank sample, where all DR-GNP-labeled antibodies are bound to the reagent forming the Test line. In conclusion, the more AFB1 presents in the sample, the lower the intensity of the color of the Test line.

For DR-GNPs the best compromise in terms of sensitivity and signal intensities was achieved by using pH 5 for conjugation to antibodies and OD 2 as the DR-GNP-Ab amount (fig. S3 and S4).

Comparing the two GNP labels, no evident differences were highlighted in terms of the behavior as a function of the pH of conjugation, provided that the same antibody was employed (fig. S5). No advantages in terms of ICST sensitivity was achieved by employing the DR-GNP label instead of the s-GNP contrarily to previous observations [11]. Moreover, the coefficients of variation of replicate measurements ranged from 0.3 to 10.8 % for the DR-GNP label and from 2.9 to 12.2 % for the s-GNP label. In conclusion, at least for the model system investigated, DR-GNPs demonstrated very similar performance compared to s-GNPs.

### *The multicolor GNP-ICST*

Once demonstrated that DR-GNPs can be employed as labels for ICST development, these blue labels were exploited in combination with red GNP for establishing a multicolor ICST for the simultaneous detection of two major food contaminants that can co-occur in crops. Mycotoxins

detection is a relevant issue for food safety assessment and the need of multiplex analytical platform for their simultaneous detection has been widely highlighted [18, 20, 30-31].

Preliminary, unwanted interactions between the two different GNP labels were excluded by TEM analysis (fig. 4 a) and by assessing that SPR bands of s- and DR-GNPs did not vary upon mixing (fig. 4 b) compared to the individual GNP spectra. Moreover, each GNP-Ab conjugate was able to selectively bind to the respective Test line when applied to immunochromatographic strips in the multiplex format (i.e.: including two Test lines, each responsive for one target mycotoxin separately, fig. 4 c). The test was designed as follows: the first Test line (T1) interacted with s-GNP-labeled antibodies (red label) and was responsive to the presence of FMs, while the second Test line (T2) interacted with DR-GNP-labeled antibodies (blue label) and was responsive to the presence of AFB1.

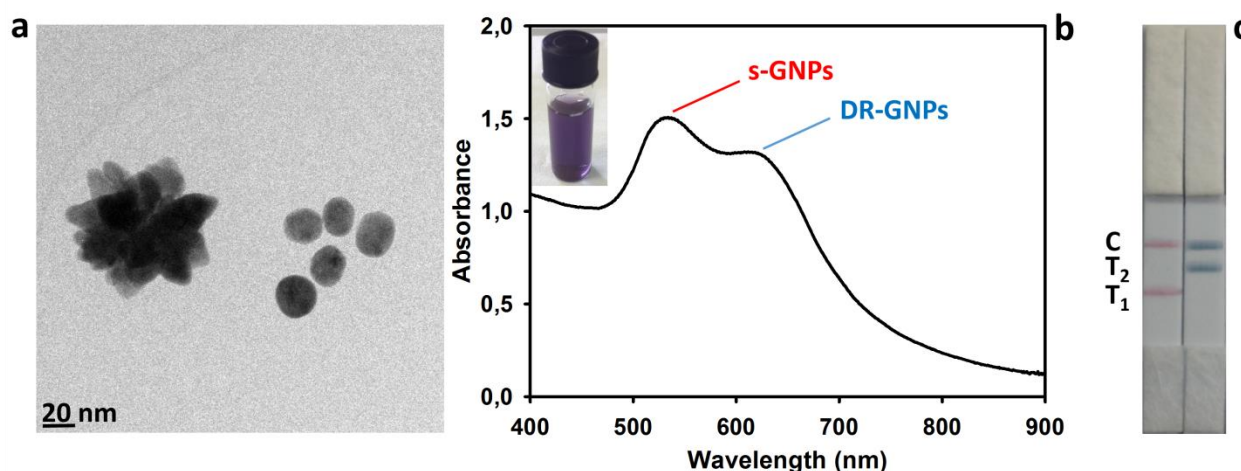


**Fig. 4.** (a) TEM micrograph of the s- and DR-GNPs mixture, obtained at 80000 x magnification. (b) Visible spectrum of the mixed s- and DR-GNPs-Ab conjugates. Inset: picture of the mixture (c) ICST results obtained by running the Ab directed towards FMB1 conjugated to the red s-GNPs (strip on the left) and the Ab directed towards AFB1 conjugated to the blue DR-GNPs (strip on the right), separately on a strip including two Test lines (T1 and T2) and a Control line (C).

Therefore, the blue DR-GNP conjugated to anti-AFB1 antibodies and the red s-GNP conjugated to anti-FMB1 antibodies were mixed and used in combination to set the multicolor ICST in the multiplex format (fig. 2). The increase of each of the target in the sample determined the decrease of the color on the corresponding line, so that a fading of the red line was attributed to a sample containing FMs above a certain value (the cut-off level) and the fading of the blue line had the same meaning but referred to the content of AFB1.

To determine the visual limit of detection (vLOD) of the multicolor ICST, AFB1 and FMB1 standard solutions (in the range 0-10 ng ml<sup>-1</sup> and 0-500 ng mL<sup>-1</sup>, respectively) were analyzed. Intensities of Test lines were observed by three operators. All subjects reported signals significantly



weaker than that of a blank sample at 0.25 ng mL<sup>-1</sup> for AFB1 and at 10 ng mL<sup>-1</sup> for FMB1 (figure 5).

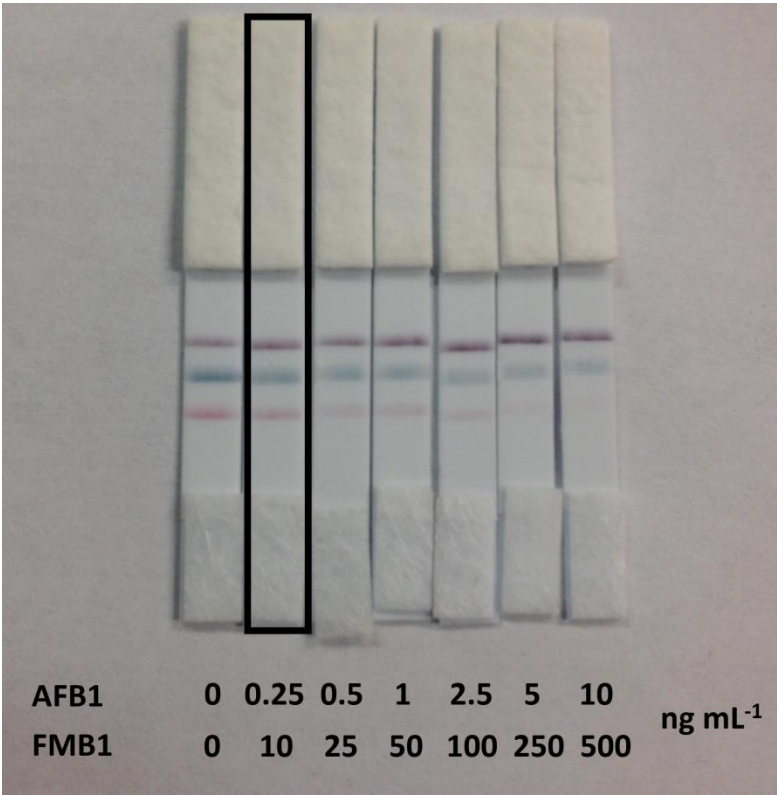


**Fig. 5.** Inhibition curve for AFB1 and FMB1. The strip corresponding to the vLODs is highlighted in black

The vLODs in maize were obtained also, by analyzing a blank sample extract fortified at four levels for each mycotoxin (0-0.2-0.4-1 ng mL<sup>-1</sup> for AFB1 and 0-50-100-200 ng mL<sup>-1</sup> for FMB1, respectively) and sorted to be 0.4 ng mL<sup>-1</sup> and 200 ng mL<sup>-1</sup> for AFB1 and FMB1 (fig. S6 and S7), corresponding to 2 µg kg<sup>-1</sup> and 1000 µg kg<sup>-1</sup> respectively in the maize flour.

The vLODs obtained in maize were set as the cut-off levels of the test. The AFB1 cut-off level corresponded to the regulatory limit decided by European Union for cereals and products derived from cereals [25]. The FMB1 cut-off level corresponded to the regulatory limit set by European Union for maize and maize-based food intended for direct human consumption [29]. Therefore, the multicolor ICST allows the simultaneous detection of AFB1 and FMB1, also fulfilling the EU legal requirements.

It is worthwhile noting that the two cut-off levels are in very different range, however the negligible cross-reactivity between AFB1 and FMB1 systems allows their correct and accurate detection.

The assay precision and accuracy were evaluated on fortified samples, prepared by adding AFB1 and FMB1 to the extract of a blank maize flour at each cut-off level separately. Fortified samples were analyzed in eight replicates and compared to the blank sample. Colors on Test lines of the



replicates were quite similar to each other and clearly differed from that produced by the blank (fig. 6).

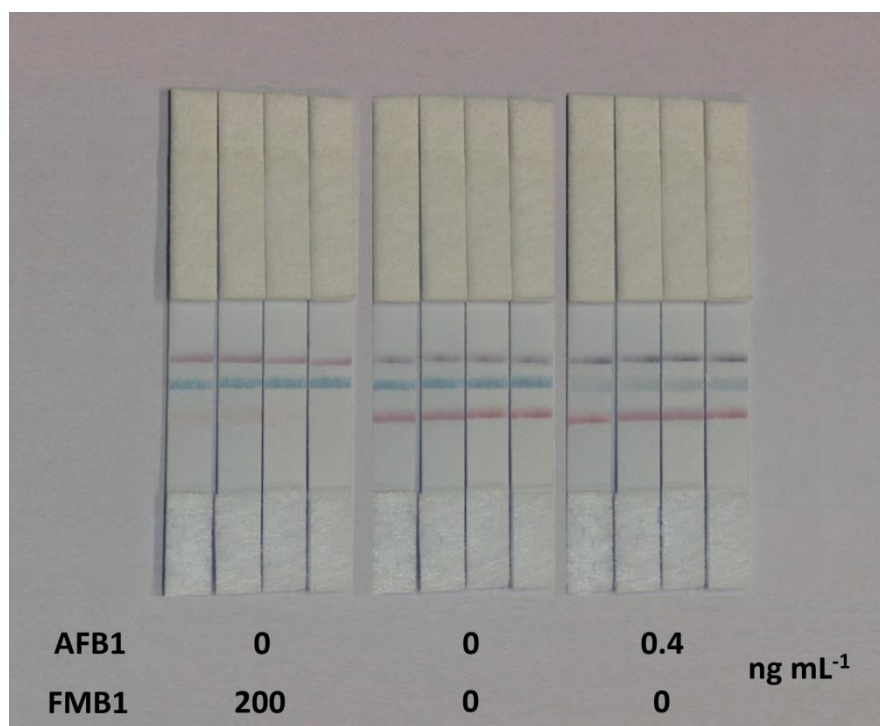


**Fig. 6.** Replicate measurements of a blank maize sample fortified with FMB1 (200 ng mL<sup>-1</sup>, left) and AFB1 (0.4 ng mL<sup>-1</sup>, right) in comparison to the raw negative sample (center). Four replicates for each sample are shown.

#### *Analysis of maize flour samples*

To evaluate further the accuracy of the method, 18 naturally contaminated maize flour samples obtained from producers or mills were qualitatively analyzed through the multicolor ICST and results were compared to those obtained by reference methods.

According to the cut-off levels defined as above described, samples containing FMs were classified as negative /positive for contamination levels below/above 1000 µg kg<sup>-1</sup>, samples containing AFB1 were classified as negative /positive for contamination levels below/ above 2 µg kg<sup>-1</sup>. Based on contamination measured by the reference methods, the 18 samples were classified as follow: 8 samples were negative both for FMs and AFB1, 4 samples were positive for FMs and negative for AFB1, and 6 samples were positive for AFB1 and negative for FMs.

Each sample was analyzed in triplicate by the multicolor ICST and judged qualitatively by the naked eye by three operators (Table S1).

A good agreement with the reference values was obtained for all samples, except for one sample (contaminated by FMs at 980 µg kg<sup>-1</sup>) that was judged differently by the three subjects involved in

the study. Since two out of three subjects judged the sample as positive; the sample was classified as false positive.

The diagnostic sensitivity and specificity were, therefore, calculated as 100% and 96.3%, respectively; the efficiency of the analytical method was 97.3%, while the positive and negative predictive values were 90.9% and 100%, respectively [38].

## **Conclusion**

Due to the growing use of the immunochromatographic technique and its expanding application in diverse fields, amelioration of its performance is strongly advisable and widely pursued. This effort is testified also by the number of papers reporting new materials to be used as labels [10-12, 39-40], sometimes in combination with innovative detection technologies [13, 41], and of enhancement strategies aimed at increasing the sensitivity of the ICST compared to using traditional gold nanoparticles [42-43], as also summarized in two comprehensive reviews [44-45]. Within the number of novel materials for labeling antibodies in ICTS, the request for analytical devices with multiplexing capability is prompting towards using labels easily distinguishable from each other, such as nanoparticles with different colors [19-20, 23]. Gold nanoparticles are widely employed as labels for ICST, thanks to well-recognized advantages, such as easy preparation, stability, easy conjugation to antibodies, brilliant and tunable color [6-8, 45]. In this paper, two kinds of GNP differing for the color were prepared and used in combination to set a simple and rapid ICST for determining two mycotoxins simultaneously. Although more sensitive assays based on the same technology have been reported for the determination of each mycotoxin separately [46], their determination in a single ICST device has not been described [47], except in a previous work of our group based on using an enzyme as the label coupled to chemiluminescent (CL) detection [48]. The CL-ICST was more sensitive and allowed for accurate and precise mycotoxin quantification, also thanks to the instrumental apparatus used for measuring and elaborating the signal. The test required 30 minutes to achieve completion (not including sample preparation) and several subsequent operations. The multicolor ICST based on GNPs is more rapid (total assay time 10 minutes) and still sufficiently sensitive and accurate for its use as a first screening tool in the food safety assessment.

## **Acknowledgements**

Authors are grateful to Dr. M. Manzoli and Prof. V. Maurino for the fruitful and helpful discussion related to the TEM and DLS measurements.

## References

- [1] Prakash J, Pivin JC, Swart HC (2015) Noble metal nanoparticles embedding into polymeric materials: From fundamentals to applications. *Adv Coll Interface Sci* 226:187-202. doi: 10.1016/j.cis.2015.10.010.
- [2] Sardar R, Funston AM, Mulvaney P, Murray RW (2009) Gold Nanoparticles: Past, Present, and Future. *Langmuir* 25:13840-13851. doi: 10.1021/la9019475.
- [3] Liu X, Wang Y, Chen P, Wang Y, Zhang J, Aili D, Liedberg B (2014) Biofunctionalized Gold Nanoparticles for Colorimetric Sensing of Botulinum Neurotoxin A Light Chain. *Anal Chem* 86:2345-2352. doi: 10.1021/ac402626g.
- [4] Gao Y, Li X, Li Y, Li T, Zhao Y, Wu A (2014) A simple visual and highly selective colorimetric detection of  $\text{Hg}^{2+}$  based on gold nanoparticles modified by 8-hydroxyquinolines and oxalates. *Chem Commun* 50:6447-6450. doi: 10.1039/c4cc00069b.
- [5] Li YS, Zhou Y, Meng XY, Zhang YY, Song F, Lu SY, Ren HL, Hu P, Liu ZS, Zhang JH (2014) Gold nanoparticle aggregation-based colorimetric assay for  $\beta$ -casein detection in bovine milk samples. *Food Chem* 162:22-26. doi: 10.1016/j.foodchem.2014.04.049.
- [6] Omidfar K, Khorsand F, Azizi MD (2013) New analytical applications of gold nanoparticles as label in antibody based sensors. *Biosens Bioelectron* 43:336-347. doi: 10.1016/j.bios.2012.12.045.
- [7] Chun P (2009) Colloidal gold and other labels for lateral flow immunoassays. In: Wong RC, Tse HY (ed) *Lateral Flow Immunoassay*, 1st edn. Humana Press, New York, pp 75-93.
- [8] Mak WC, Beni V, Turner APF (2016) Lateral-flow technology: From visual to instrumental. *TrAC Trends Anal Chem* 79: 297-305. doi: 10.1016/j.trac.2015.10.017.
- [9] Han S, Zhou T, Yin B, He P (2016) A sensitive and semi-quantitative method for determination of multidrug residues in animal body fluids using multiplex dipstick immunoassay. *Anal Chim Acta* 927: 64-71. doi: 10.1016/j.aca.2016.05.004.
- [10] Zhang L, Huang Y, Wang J, Rong Y, Lai W, Zhang J, Chen T (2015) Hierarchical flowerlike gold nanoparticles labeled immunochromatography test strip for highly sensitive detection of *Escherichia coli* O157:H7. *Langmuir* 31:5537-554
- [11] Ji Y, Ren M, Li Y, Huang Z, Shu M, Yang H, Xiong Y, Xu Y (2015) Detection of aflatoxin B1 with immunochromatographic test strips: Enhanced signal sensitivity using gold nanoflowers. *Talanta* 142: 206-212. doi:10.1016/j.talanta.2015.04.048
- [12] Wiriyachaiporn, N., Maneeprakorn, W., Apiwat, C., & Dharakul, T. (2015). Dual-layered and double-targeted nanogold based lateral flow immunoassay for influenza virus. *Microchimica Acta*, 182:85-93.

- [13] Man, Y., Lv, X., Iqbal, J., Peng, G., Song, D., Zhang, C., & Deng, Y. (2015). Microchip based and immunochromatographic strip assays for the visual detection of interleukin-6 and of tumor necrosis factor  $\alpha$  using gold nanoparticles as labels. *Microchim Acta*, 182:597-604
- [14] Luan Y, Chen J, Xie, G, Li, C, Ping H, Ma Z, Lu A. (2015). Visual and microplate detection of aflatoxin B2 based on NaCl-induced aggregation of aptamer-modified gold nanoparticles. *Microchim Acta*, 182:995-1001
- [15] Lu Z, Chen X, Wang Y, Zheng X, Li CM (2015) Aptamer based fluorescence recovery assay for aflatoxin B1 using a quencher system composed of quantum dots and graphene oxide. *Microchim Acta*, 182:571-578.
- [16] Brown MC (2009) Antibodies: key to a robust lateral flow immunoassay. In: Wong RC, Tse HY (ed) *Lateral Flow Immunoassay*, 1st edn. Humana Press, New York, pp 59-74.
- [17] O'Farrell B (2015) Lateral Flow Technology for Field-Based Applications-Basics and Advanced Developments. *Topics Compan Anim Med* 30:139–147. doi: 10.1053/j.tcam.2015.12.003.
- [18] Anfossi L, Giovannoli C, Baggiani C (2016) Mycotoxin detection. *Curr Opin Biotechnol* 37:120-126. doi: 10.1016/j.copbio.2015.11.005.
- [19] Taranova NA, Berlina AN, Zherdev AV, Dzantiev BB (2014) 'Traffic light' immunochromatographic test based on multicolor quantum dots for the simultaneous detection of several antibiotics in milk. *Biosens Bioelectron* 63:255-61. doi: 10.1016/j.bios.2014.07.049
- [20] Foubert A, Beloglazova NV, Gordienko A, Tessier MD, Drijvers E, Hens Z, De Saeger S. (2016) Development of a Rainbow Lateral Flow Immunoassay for the Simultaneous Detection of Four Mycotoxins. *J Agric Food Chem*. doi: 10.1021/acs.jafc.6b04157
- [21] Li J, Wu J, Zhang X, Liu Y, Zhou D, Sun H, Zhang H, Yang B (2011) Controllable Synthesis of Stable Urchin-like Gold Nanoparticles Using Hydroquinone to Tune the Reactivity of Gold Chloride. *J Phys Chem C* 115:3630-3637. doi: 10.1021/jp1119074
- [22] Zhao L, Ji X, Sun X, Li J, Yang W, Peng X (2009) Formation and Stability of Gold Nanoflowers by the Seeding Approach: The Effect of Intraparticle Ripening. *J Phys Chem C* 113:16645-16651. doi: 10.1021/jp9058406
- [23] Yen CW, de Puig H, Tam JO, Gómez-Márquez J, Bosch I, Hamad-Schifferli K, Gehrke L (2015) Multicolored silver nanoparticles for multiplexed disease diagnostics: distinguishing dengue, yellow fever, and Ebola viruses. *Lab Chip* 15:1638-1641. doi: 10.1039/c5lc00055f
- [24] International Agency for Research on Cancer (2002) Evaluation of carcinogenic risks in humans. 82: 171–274.
- [25] Commission Regulation (EU) No 165/2010, Off J Eur Comm, L50, 8-12.

- [26] Di Nardo F, Anfossi L, Giovannoli C, Passini C, Gofmann VV, Goryacheva IY, Baggiani C (2016) A fluorescent immunochromatographic strip test using Quantum Dots for fumonisins detection. *Talanta* 150: 463-468. doi: 10.1016/j.talanta.2015.12.072
- [27] Marasas W F O (2001) Discovery and occurrence of the fumonisins: a historical perspective. *Environmental Health Perspectives* 109: 239-243. doi: 10.2307/3435014.
- [28] International Agency for Research on Cancer (1993). Monographs on the evaluation of the carcinogenic risk of chemicals to humans 82: 301–366.
- [29] Commission Regulation (EC) No. 1126/2007, Off. J. Eur. Comm., L255, 14–17.
- [30] Goryacheva I Y, De Saeger S, Eremin S A, Van Peteghem C (2007) Immunochemical methods for rapid mycotoxin detection: Evolution from single to multiple analyte screening: A review. *Food Addi Contam A* 24:1169–1183. doi: 10.1080/02652030701557179.
- [31] Krska R, Schubert-Ullrich P, Molinelli A, Sulyok M, MacDonald S, Crews C (2008) Mycotoxin analysis: An update. *Food Add Contam A* 25:152-163. doi: 10.1080/02652030701765723.
- [32] Anfossi L, Calderara M, Baggiani C, Giovannoli C, Arletti E, Giraudi G (2010) Development and application of a quantitative lateral flow immunoassay for fumonisins in maize. *Anal Chim Acta* 682: 104–109. doi:10.1016/j.aca.2010.09.045
- [33] Khlebstov N G (2008) Determination of Size and Concentration of Gold Nanoparticles from Extinction Spectra. *Anal Chem* 80: 6620-6625. doi:10.1021/ac800834n.
- [34] Jazayeri M H, Amani H, Pourfatollah A, Pazoki-Toroudi H, Sedighimoghaddam B (2016) Various methods of gold nanoparticles (GNPs) conjugation to antibodies. *Sens Biosensing Res* 9: 17–22. doi: 10.1016/j.sbsr.2016.04.002.
- [35] Daohong Zhang D, Li P, Zhang Q, Zhang W (2011) Ultrasensitive nanogold probe-based immunochromatographic assay for simultaneous detection of total aflatoxins in peanuts. *Biosens Bioelectron* 26: 2877–2882. doi:10.1016/j.bios.2010.11.031
- [36] Oliver C (2010) Conjugation of colloidal gold to proteins. *Meth Mol Biol* 588:369-73. doi: 10.1007/978-1-59745-324-0\_39.
- [37] Majdinasab M, Sheikh-Zeinoddin M, Soleimanian-Zad S, Li P, Zhang Q, Li X, Tang X (2015) Ultrasensitive and quantitative gold nanoparticle-based immunochromatographic assay for detection of ochratoxin A in agro-products. *J Chromatogr B* 974: 147-154. doi: 10.1016/j.jchromb.2014.10.034.

- [38] Di Nardo F, Anfossi L, Ozella L, Saccani A, Giovannoli C, Spano G, Baggiani C (2016) Validation of a qualitative immunochromatographic test for the noninvasive assessment of stress in dogs. *J Chromatogr B* 1028: 192-198. doi: 10.1016/j.jchromb.2016.06.019.
- [39] Li Z, Wang Y, Wang J, Tang Z, Pounds JG, Lin Y (2010) Rapid and Sensitive Detection of Protein Biomarker Using a Portable Fluorescence Biosensor Based on Quantum Dots and a Lateral Flow Test Strip. *Anal Chem* 82:7008–7014 doi: 10.1021/ac101405a
- [40] Tatona K, Johnsona D, Guirea P, Langeb E, Tondra (2009) M Lateral flow immunoassay using magnetoresistive sensors. *J Magn Magn Mater* 321:1679–1682
- [41] Du D, Wang J, Wang L, Lu D, Lin Y (2012) Integrated Lateral Flow Test Strip with Electrochemical Sensor for Quantification of Phosphorylated Cholinesterase: Biomarker of Exposure to Organophosphorus Agents. *Anal Chem* 84:1380–1385
- [42] Parolo C, de la Escosura-Muñiza A, Merkoçi A (2013) Enhanced lateral flow immunoassay using gold nanoparticles loaded with enzymes. *Biosens Bioelectron* 40:412-416
- [43] Rivas L, de la Escosura-Muñiz A, Serrano L, Altet L, Francino O, Sánchez A, Merkoçi A (2015) Triple lines gold nanoparticle-based lateral flow assay for enhanced and simultaneous detection of *Leishmania* DNA and endogenous control. *Nano Res* 8:3704-3714
- [44] Quesada-González D, Merkoçi A (2015) Nanoparticle-based lateral flow biosensors. *Biosens Bioelectron* 73:47-63
- [45] Sajid M, Kawde A-N, Daud M (2015) Designs, formats and applications of lateral flow assay: A literature review. *J Saudi Chem Soc* 19:689–705
- [46] Chauhan R, Singh J, Sachdev T, Basu T, Malhotra BD. (2016) Recent advances in mycotoxins detection. *Biosens Bioelectron* 81:532-545. doi: 10.1016/j.bios.2016.03.004
- [47] Maragos CM (2016) Multiplexed Biosensors for Mycotoxins. *J AOAC Int* 99: 849-860
- [48] Zangheri M, Di Nardo F, Anfossi L, Giovannoli C, Baggiani C, Roda A, Mirasoli M (2015) A multiplex chemiluminescent biosensor for type B-fumonisins and aflatoxin B1 quantitative detection in maize flour. *Analyst* 140:358-65. doi: 10.1039/c4an01613k